Discovery of (S)-1-(1-(4-Chloro-3-fluorophenyl)-2-hydroxyethyl)-4-(2-((1-methyl-1H-pyrazol-5-yl)amino)pyrimidin-4-yl)pyridin-2(1H)-one (GDC-0994), an Extracellular Signal-Regulated Kinase 1/2 (ERK1/2) Inhibitor in Early Clinical Development

James F. Blake,[†] Michael Burkard,[†] Jocelyn Chan,[‡] Huifen Chen,[‡] Kang-Jye Chou,[‡] Dolores Diaz,[‡] Danette A. Dudley,[‡] John J. Gaudino,[†] Stephen E. Gould,[‡] Jonas Grina,[†] Thomas Hunsaker,[‡] Lichuan Liu,[‡] Matthew Martinson,[†] David Moreno,[†] Lars Mueller,[‡] Christine Orr,[‡] Patricia Pacheco,[‡] Ann Qin,[‡] Kevin Rasor,[†] Li Ren,[†] Kirk Robarge,[‡] Sheerin Shahidi-Latham,[‡] Jeffrey Stults,[‡] Francis Sullivan,[†] Weiru Wang,[‡] Jianping Yin,[‡] Aihe Zhou,[‡] Marcia Belvin,[‡] Mark Merchant,[‡] John Moffat,[‡] and Jacob B. Schwarz*,[‡]

[†]Array BioPharma Inc., 3200 Walnut Street, Boulder, Colorado 80301, United States
[‡]Genentech, Inc., 1 DNA Way, South San Francisco, California 94080, United States

S Supporting Information

ABSTRACT: The extracellular signal-regulated kinases ERK1/2 represent an essential node within the RAS/RAF/MEK/ERK signaling cascade that is commonly activated by oncogenic mutations in BRAF or RAS or by upstream oncogenic signaling. While targeting upstream nodes with RAF and MEK inhibitors has proven effective clinically, resistance frequently develops through reactivation of the pathway. Simultaneous targeting of multiple nodes in the pathway, such as MEK and ERK, offers the prospect of enhanced efficacy as well as reduced potential for acquired resistance. Described herein is the discovery and characterization of GDC-0994 (**22**), an orally bioavailable small molecule inhibitor selective for ERK kinase activity.
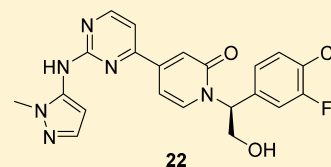
The RAS/RAF/MEK/ERK (MAPK) signal transduction pathway is widely activated in a large subset of human cancers and thus has attracted significant interest as a therapeutic target for cancer.[1] Constitutive activation of the MAPK pathway by oncogenic RAS and RAF mutations as well as activation or overexpression of growth factor receptors results in sustained activation of the central effector kinases ERK1 and ERK2 (MAPK3 and MAPK1). ERK1/2 phosphorylates more than 50 downstream substrates responsible for cell growth, proliferation, survival, angiogenesis, and differentiation.[2-4]

Small molecule inhibitors of BRAF and MEK have shown promising activities in the clinic for a variety of solid tumors. The approval of vemurafenib,[5] dabrafenib,[6] trametinib,[7] and cobimetinib[8] as treatments for BRAF-mutant metastatic melanoma validates the approach of targeting the MAPK pathway as an effective way of treating cancer. However, these agents can show limitations in duration of efficacy for some patients due to the acquisition of pathway-reactivating mutations.[9] Further, outside this indication, the efficacy of these agents has been disappointing, despite apparent MAPK pathway activation and clear therapeutic rationale in BRAF or RAS mutant cancers. Negative feedback loops within the MAPK pathway enable pathway reactivation when targeted with inhibitors of single nodes, driving innate insensitivity of RAS mutant tumors to MEK inhibitors and of some BRAF mutant tumors (e.g., colorectal) to BRAF or MEK inhibitors.[10]

Even when tumors respond to therapy, acquired resistance to receptor tyrosine kinase (RTK) BRAF or MEK inhibitors can limit durable responses, many of which involve bypass or reactivation of the drug target and restoration of persistent MAPK activation resulting in high ERK activity.[11]

Downstream of MEK, the ERK kinases represent the final single node that would be expected to suppress MAPK signaling. ERK1/2 inhibitors are effector kinases for the MAPK pathway that are responsible for phosphorylating multiple targets to drive gene transcription and protein translation to enable cell growth. Targeting ERK is therefore expected to directly suppress the effector node of the MAPK pathway and potentially address acquired or innately resistant tumors.[12] ERK inhibitors could further combine with drugs targeting upstream nodes in the MAPK pathway to drive deeper pathway suppression and reduce the incidence of acquired resistance.[13] Herein we report the optimization of preclinical potency, selectivity, and pharmacology parameters resulting in the discovery of (S)-1-(1-(4-chloro-3-fluorophenyl)-2-hydroxyethyl)-4-(2-((1-methyl-1H-pyrazol-5-yl)amino)pyrimidin-4-yl)-pyridin-2(1H)-one (**22**), which was advanced to human clinical trials.
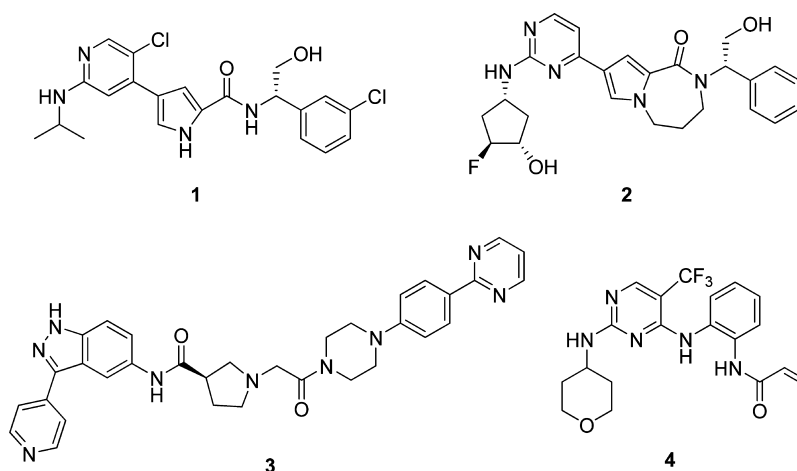
Figure 1. Highly optimized ERK inhibitors.

ERK has been a long-standing target in the pharmaceutical industry, and several highly optimized inhibitors have been reported.[14] One of the first examples of potent, selective ERK inhibitors was a pyrrole-based series from Vertex that appeared in 2007.[15] A compound that emerged from this work, BVD-523 **1**, is currently being studied in early clinical development by Biomed Valley Discoveries (Figure 1).[16] Cyclized variants of **1**, represented by **2**, were recently disclosed by researchers at Novartis.[17] Merck reported in 2013 that the linear indazole **3** (SCH772984) displayed behaviors typical of both type I and type II kinase inhibitors.[18] More recently, covalent ERK2 inhibitors such as **4** have been disclosed by AstraZeneca.[19]

We have previously reported the discovery of novel, potent, and selective ERK1/2 inhibitors based on piperidinopyrimidine[20] and pyridone[21] scaffolds, as typified by compounds **5** and **6**. While compound **6** in particular possessed a number of desirable attributes, some critical features were identified for further optimization. The human dose projection for **6** based on PK/PD modeling of the mouse xenograft data and allometric scaling was considered to be unacceptably high (>1 g/day),[22] and therefore a strategy to reduce the predicted compound load was developed. Two specific areas for optimization were targeted: improved potency and improved exposure. For the former, recourse to structure-based drug design was available for enhancing potency against ERK1/2. For the latter, we initiated the investigation by considering the metabolic fate of the lead pyridone **6**.
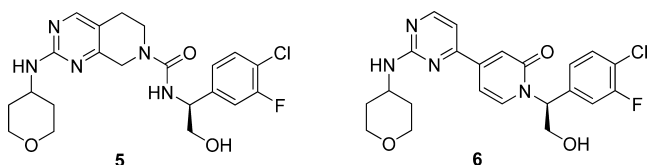
Compound **6** was incubated with human, mouse, dog, rat, and cynomolgus monkey hepatocytes for 3 h and the metabolite profile examined by LC−MS/MS (Figure 2). In all species metabolism occurred primarily on the tetrahydropyran (THP) ring, and the major product was determined to be hydroxy acid **7**. In vivo metabolism studies with **6** in rat, dog, and monkey confirmed **7** to be the primary circulating species in plasma as well as urine. Clearly, substitution or outright replacement of the THP moiety would be key to any strategy to enhance the metabolic stability. A number of saturated aliphatic

and cyclic THP replacements of **6** were reported previously,[20] but unfortunately none of these resulted in improved metabolic stability. Heteroaromatic replacements were considered to eliminate the methylene soft spots of **6**. Importantly, the hydrogen bond accepting nature of the THP oxygen atom was a key potency driver for **6** and would need to be preserved in order to maintain the crucial hydrogen bond interaction with Lys114 of ERK2, thereby considerably limiting the number of suitable candidate motifs.
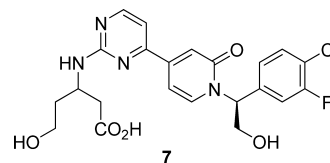
THP replacement analogs were prepared by the methods previously described.[20,23] Hence, TBS-protected sulfone **8** was subjected to S_NAr displacement aided by deprotonation of or heating with the appropriate amino heterocycle (Figure 3). Subsequent deprotection of the silyl protecting group with TBAF or HCl in organic solvent afforded compounds **9**−**28** for evaluation. The first THP replacement that was investigated was 2-methylpyridine **9**. The pyridine nitrogen atom was expected to form a hydrogen bond with the Lys114 side chain. The methyl group was incorporated to thwart potential metabolism at the pyridyl nitrogen atom. Although the mechanistic cell potency of the compound (inhibition of ERK-dependent p90RSK phosphorylation, pRSK) was outstanding, the compound was a potent CYP3A4 inhibitor (IC$_{50}$ = 0.34 μM). In addition, compound **9** showed high clearance and low bioavailability in rat, thereby eliminating it from consideration for further development. Utilization of alternate pyridine substitution patterns or adding or reorganizing heteroatoms in the ring did not afford any useful attenuation of CYP3A4 activity without concomitant loss in activity (data not shown). As a result, we turned our attention toward THP replacement by five-membered ring motifs.

The first replacement of the aminopyridine in **9** to be studied was 4-aminopyrazole. On the basis of molecular modeling, 4-pyrazoles would present a hydrogen bond acceptor in an ideal orientation to interact with the Lys114 side chain while also providing vectors suitable for substitution to improve selectivity. A number of analogs with subtle alkyl modifications
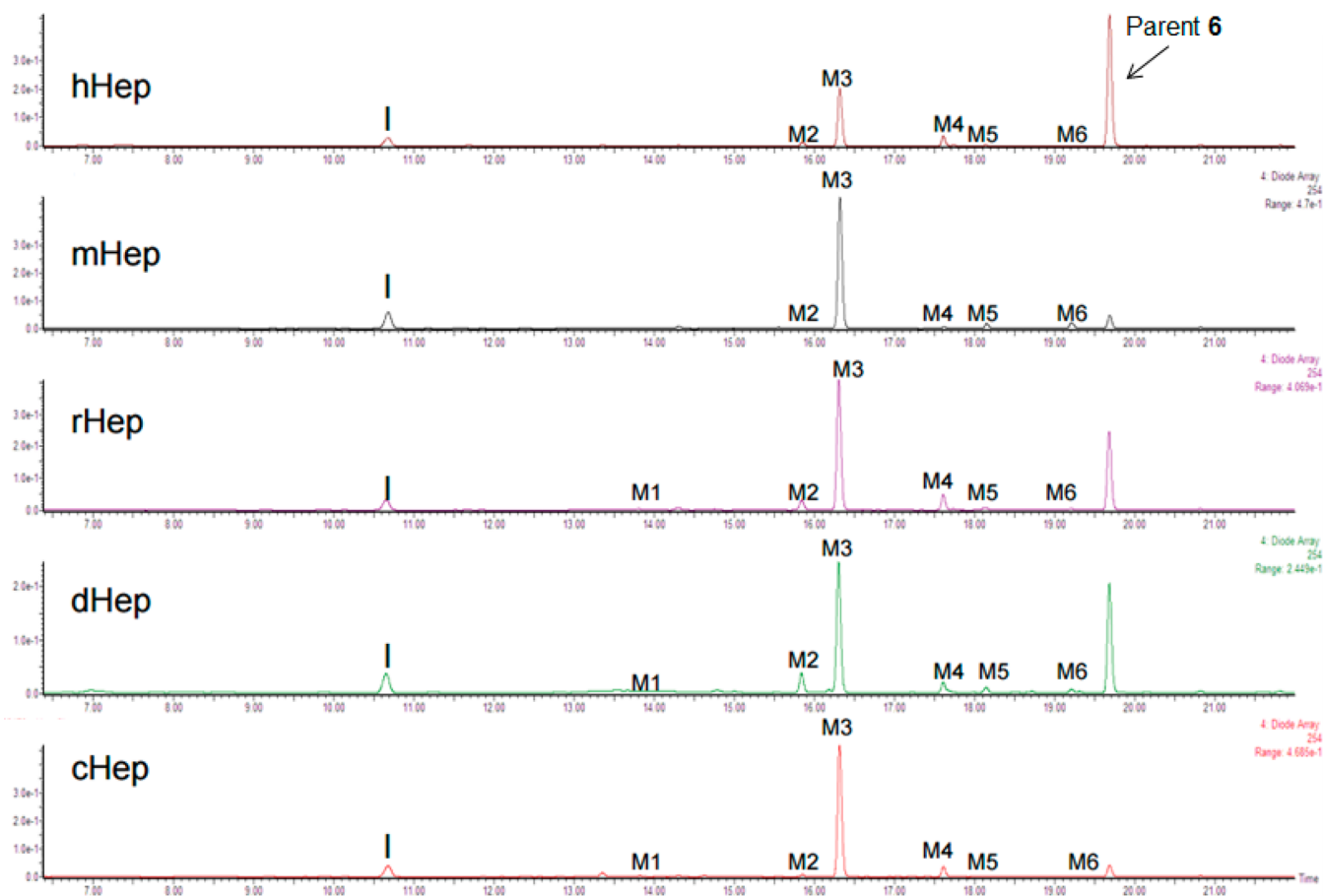
Figure 2. UV traces from incubation of **6** with hepatocytes at t = 3 h (M3 = compound **7**): h = human, m = mouse, r = rat, d = dog, c = cynomolgus monkey. The most abundant metabolites M1−M6 are labeled. The first peak common to all five traces represents an internal standard.
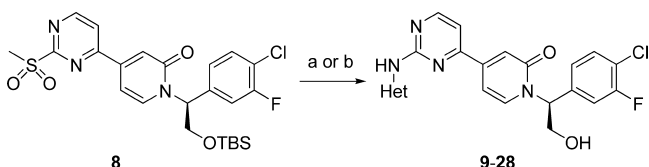

Figure 3. Synthesis of THP replacement analogs **9**−**28**. Conditions are the following. (a) For 4-aminopyrazoles: (i) Het-NH$_2$, s-BuOH, 120 °C; (ii) TBAF, THF. (b) For 5-aminopyrazoles: (i) NaH, DMF, rt or 150 °C; HCl, EtOAc.

were synthesized and tested (Table 1). Compounds were screened for enzyme potency against ERK1 and ERK2, mechanistic potency in HepG2 cells, and metabolic stability in the presence of human microsomes. The simple N-methylated pyrazole **10** showed enzyme and cell potency similar to **6**, but adding a second methyl to the adjacent position as in **11** resulted in a sharp decline in activity. However, if the second methyl was added to the other available carbon as in **12**, not only was potency restored but an enhancement of selectivity against the cell cycle kinase CDK2 was observed. CDK2 was chosen as the primary antitarget kinase to screen based on its close homology in the binding site to ERK2 (vide infra) and the observation that it was consistently more strongly inhibited than other members of the CDK family in kinase selectivity profiling (not shown). The enhanced selectivity of **12** against CDK2 may be attributed to the C-3 methyl group which was predicted by docking to point toward the ERK2 Leu107 and insult the larger Phe82 side chain

in CDK2. Extension of the C-methyl group of **12** as in **13** resulted in loss of potency due to steric clash with the protein, although extension of the N-methyl group (**14**) was tolerated. Deletion of the C-methyl group of **14** as in **15** brought back potency but imparted loss of selectivity, allowing for the conclusion that the C-methyl substituent was a key selectivity driver. Bulking up the N-substitution of **15** to isopropyl in **16** resulted in lower potency. In contrast, when the N-substituent of **12** was removed altogether, a potent and selective compound **17** was obtained. Having two C-methyl groups on the pyrazole as in **18** was not tolerated, which was also the case for trifluoromethyl substituted **19**. Noteworthy was the fact that the pyrazoles did not demonstrate potent inhibition of the various CYP enzymes, unlike pyridine **9** (data not shown).

Given the similarity in vitro of compound **12** to the previous lead compound THP **6**, a PK study was performed in CD-1 mice. Although the clearance was similar for both compounds (extraction ratio ∼30%), pyrazole **12** showed greater oral bioavailability (95% vs 66% for **6**), rationalizing further investment in this series to increase potency. Armed with this promising result, a series of substituted 5-aminopyrazoles was investigated (Table 2). The SAR generally tracked with the 4-aminopyrazole series, but the direct comparator to **12** (compound **24**) was roughly 2-fold less potent in cells. There was, however, a clear standout from the series in terms of cell potency which was N-methylpyrazole **22**. It was 10-fold more potent in cells than the next most potent compound (**26**) in the series. It was also 5-fold more potent in cells than

Table 1. Pyridine and 4-Aminopyrazole Derivatives
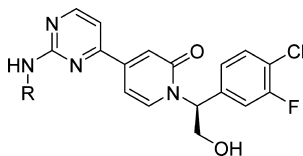
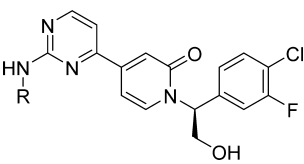| Cpd	R	ERK1 IC$_{50}$ nM (95% CI)[a]	ERK2 IC$_{50}$ nM (95% CI)	CDK2 /ERK2[b]	p-RSK IC$_{50}$ (nM)[c]	HLM CL$_{hep}$ (mL/min/kg)[d]
6		2.7 (2.4, 3.0)	1.1 (0.77, 1.6)	16	49	9
9		3.9 (3.2, 4.7)	0.94 (0.54, 1.6)	14	8	11
10		7.9 (7.3, 8.5)	4.1 (2.7, 5.9)	14	44	11
11		62 (53, 71)	29 (18, 47)	14	530	14
12		13 (11, 15)	5.9 (4.5, 7.8)	54	64	16
13		43 (36, 50)	23 (19, 28)	28	230	18
14		18 (10, 30)	7.7 (2.9, 20)	55	100	18
15		5.0 (4.0, 6.1)	1.8 (0.92, 3.6)	14	34	15
16		19 (18, 21)	10 (5.5, 18)	9.5	127	17
17		3.8 (1.9, 7.6)	0.9 (0.7, 1.0)	65	38	9
18		510 (350, 720)	240 (190, 290)	3.5	5,000	12
19		550 (430, 710)	290 (180, 470)	--	3,500	8

[a]Enzyme potency against ERK1 ($n > 2$ with 95% confidence interval). [b]Ratio of CDK2 IC$_{50}$ to ERK2 IC$_{50}$. [c]Inhibition of ERK dependent p90RSK serine 380 phosphorylation in PMA-stimulated HepG2 cells. [d]Human hepatic clearance predicted from liver microsomes.
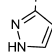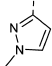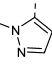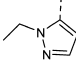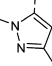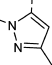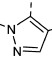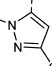
compound **12**. In addition, it was moderately stable when incubated with human liver microsomes. As a result, we decided to more fully profile compound **22** as a potential development candidate.

To fully characterize the binding interactions, we determined a cocrystal structure of **22** and ERK2. The overall binding mode is consistent with the predicted docking pose, largely resembling that of **6** (PDB code 5K4I).[21] The 2-amino-pyrimidine interacts with the hinge region of ERK2 at Met108 and Leu107 by forming a pair of H-bonds (Figure 4A). The

pyridone carbonyl makes water mediated H-bonds with gatekeeper Gln105 and catalytic Lys54. The hydroxymethyl group is within H-bond distance from the side chains of Asp167 and Asn154. The fluorochlorophenyl terminal group binds to a hydrophobic pocket under the glycine-rich loop that involves the side chain of Tyr36. The 5-amimopyrazole accepts an H-bond from Lys114, providing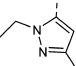 the same interaction as the THP oxygen. Comparison with a crystal structure of CDK2 in complex with **22** (PDB code 5K4J) helped to illustrate the origin of selectivity within the pyrazole series (Figure 4B).[24]

Table 2. 5-Aminopyrazole Derivatives

Cpd	R	ERK1 IC$_{50}$ nM (95% CI)[a]	ERK2 IC$_{50}$ nM (95% CI)	CDK2 /ERK2[b]	p-RSK IC$_{50}$ (nM)[c]	HLM CL$_{hep}$ (mL/min/kg)[d]
20		9,610 (8,390, 10,990)	5,650 (4,270, 7,480)	--	5,000	2
21		85 (67, 110)	37 (28, 49)	50	298	6
22		6.1 (5.0, 7.4)	3.1 (1.8, 5.5)	25	12	8
23		26 (18, 37)	16 (8.9, 31)	107	247	9
24		20 (17, 23)	13 (7, 25)	20	129	10
25		150 (110, 210)	89 (51, 150)	19	2500	13
26		27 (26, 27)	17 (9.8, 28)	17	132	15
27		1,070 (580, 1,980)	490 (430, 550)	2.7	5000	17
28		74 (54, 100)	52 (36, 74)	7.2	635	8

[a]Enzyme potency against ERK1 ($n > 2$ with 95% confidence interval). [b]Ratio of CDK2 IC$_{50}$ to ERK2 IC$_{50}$. [c]Inhibition of ERK dependent p90RSK serine 380 phosphorylation in PMA-stimulated HepG2 cells. [d]Human hepatic clearance predicted from liver microsomes.
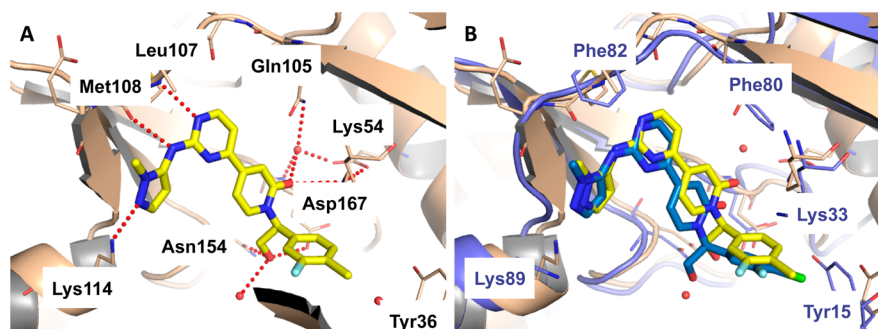
Figure 4. Crystal structures of **22** bound to ERK2 (brown) and CDK2 (purple): (A) compound **22** bound to ERK2; (B) superposition of ERK2 and CDK2 cocrystal structures with compound **22**. Red dotted lines indicate hydrogen bonds. Red spheres indicate water molecules.

This improved selectivity against CDK2 may be attributed to the N-methyl group which was predicted to point toward the Phe82 residue in CDK2, which is the counterpart of a less sterically demanding Leu107 in ERK2. The N-methyl group on the pyrazole insults the Phe82 side chain but is better tolerated by ERK2.[25] Additionally, the ERK2 gatekeeper residue Gln105 (which is very rare among kinases) is replaced by Phe80 in CDK2 rendering CDK2 devoid of the polar interactions near the gatekeeper. The structure of **22** also shifts toward the bulk solvent region in CDK2 structure relative to its position in

Figure 5. Activity of **22** against 279 kinases at 1 μM. Illustration reproduced courtesy of Cell Signaling Technology (www.cellsignal.com).

ERK2, thereby compromising the interactions around the hydroxymethyl linker and the fluorochlorophenyl terminal group. This positional shift of **22** also affects its interaction with Lys89 of CDK2, the equivalent residue to Lys114 in ERK2. The side chain of Lys89 adopts a rotamer that avoids clashing into the ligand but loses the hydrogen bond with the 5-aminopyraz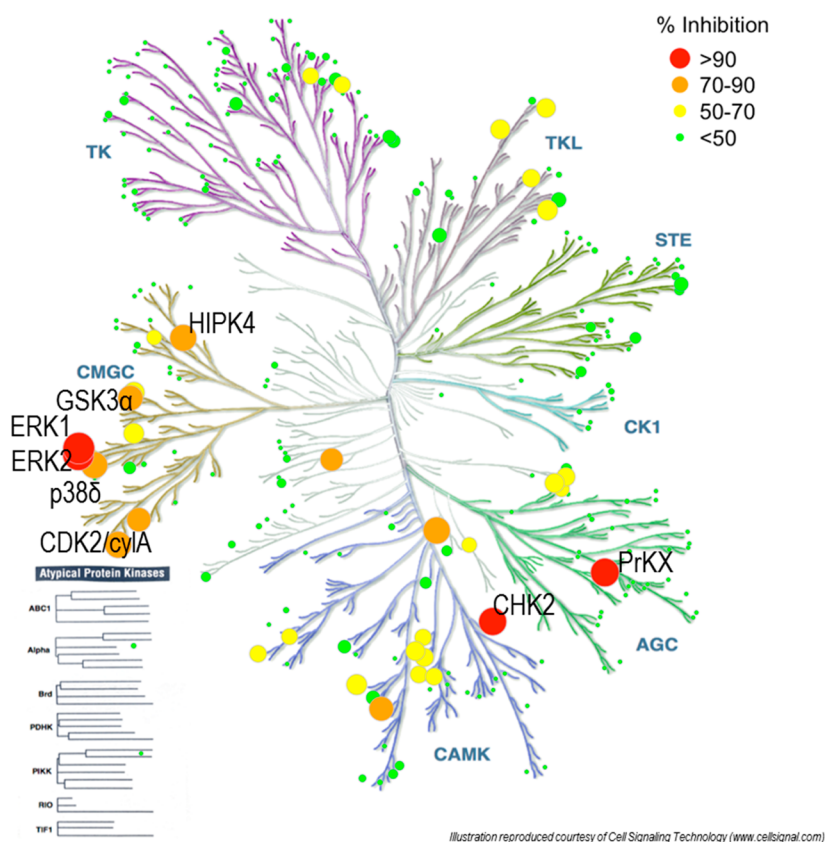ole. We reason that these multiple critical distinctions in **22** interactions with ERK2 versus CDK2 collectively contribute to the overall selectivity.

Next, the broad kinase selectivity of **22** was evaluated at 1 μM against the Invitrogen Selectscreen panel containing 279 kinases (Figure 5). The top hits were subjected to follow-up IC$_{50}$ generation. For all seven kinases identified as potential selectivity flags, at least 50-fold selectivity was observed relative to ERK1 IC$_{50}$ (Table 3).

Having identified compound **22** as having the best mix of potency and selectivity, we set out to evaluate its DMPK properties. Compound **22** demonstrated kinetic solubility and permeability in MDCK cells similar to previous lead compound **6** (29.7 μg/mL, AB = 3.9 × 10^{-6} cm/s). Taking into account

that the free fraction in mouse plasma was determined to be 5.8%, the target coverage for efficacy in a mouse xenograft study (pRSK IC$_{50}/f_u$) was calculated to be ∼200 nM total concentration in plasma. In CD-1 mice, a 10 mg/kg oral dose of **22** was sufficient to achieve the desired target coverage for at least 8 h (Figure 6).[26] For comparison, a plasma concentration of ∼2 μM for THP **6** would be required for 8 h to achieve the same target coverage, which was only achievable using a 60 mg/kg po dose.[21]

Next, iv/oral crossover PK was surveyed in rat, dog, and cynomolgus monkey (Table 4). Interestingly, the in vivo clearance measured across species was well predicted by in vitro incubation with hepatocytes, whereas liver microsomes tended to overpredict the clearance for compound **22**. Higher clearance was observed exclusively in cynomolgus monkey (extraction ratio of ∼80%). Cross-species metabolite identification in hepatocytes showed very little metabolism except in cynomolgus monkey, where the major product was shown to be glucuronidation (93% vs 5% in human). With the exception of cynomolgus monkey, the in vivo clearance values were significantly lower than those observed for compound **6**. Given the high predictive value of in vitro clearance hepatocytes for compound **22**, clearance in human was projected to be low (<5 mL min^{-1} kg^{-1}).

As a result of the promising PK data, **22** was progressed into in vivo PK/PD and efficacy studies. The HCT116 human colorectal cancer xenograft model was selected as representative of KRAS mutant cancer, which is both a "higher bar" and more representative of the likely clinical indication than BRAF mutant melanoma. A PK/PD study (15, 30, and 100 mg/kg, q.d.) was carried out in nude mice bearing subcutaneous HCT116 tumors. Significant inhibition of pRSK was observed

Table 3. Kinase Selectivity of Compound 22

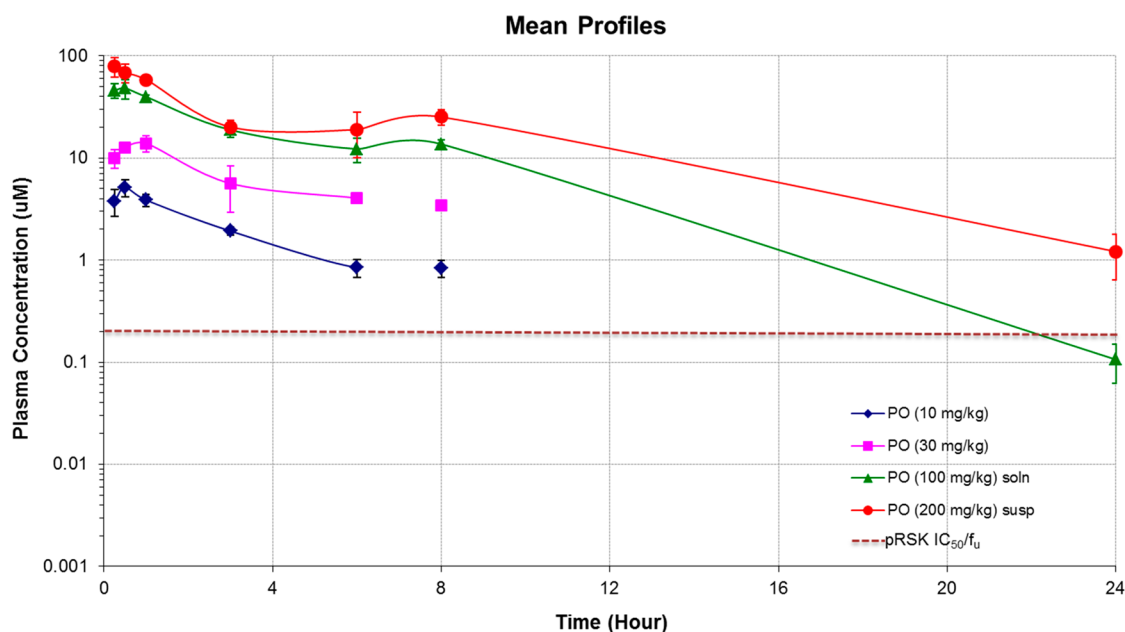| kinase	fold selectivity vs ERK1
PrKX	50
GSK3α	121
CHK2	118
HIPK4	150
P38δ	158
Cdk2/CyA	167
Aurora A	217

Figure 6. Compound exposure vs time in a multidose mouse PK study with compound **22**, formulated in 40% PEG400/60% (10% HPβCD) water.

Table 4. Pharmacokinetic Parameters of Compound 22

	rat	mouse	dog	cyno	human
in vitro predicted CL					
liver microsomes (mL min^{-1} kg^{-1})	23	48	15	23	7.9
hepatocytes (mL min^{-1} kg^{-1})	14	19	5.4	35	4.7
PPB (f_u)	0.044	0.058	0.098	0.056	0.080
in vivo PK					
CL$_p$ (mL min^{-1} kg^{-1})	15	19	6.4	31	
V_{ss} (L/kg)	1.8	1.6	2.1	2.5	
t$_{1/2,iv}$ (h)	2.0	1.3	6.8	2.4	
F (%)	35	39	112	15	
AUC/D$_{po}$ (kg·h/L)	0.41	0.54	3.8	0.09	

at the 30 and 100 mg/kg doses, with the corresponding pRSK knockdown at the 2 h time point observed to be 65% and 87% (Figure 7). As was observed previously for compound **6**,[21] there was an apparent rebound to above baseline levels in phosphorylation of p90RSK at 16 and 24 h for **22** (Figure 7). Pathway reactivation and rebound transiently above basal levels correlate with decreased drug exposure and are consistent with rebound effects observed with other MAPK inhibitors. Next, compound **22** was evaluated in a proof-of-concept tumor growth inhibition (TGI) study. The compound was administered once daily (q.d.) orally for 21 days in nude mice bearing HCT116 human colorectal cancer subcutaneously implanted xenograft tumors (Figure 8). At doses greater than 30 mg/kg, there was significant tumor growth inhibition with 30, 60, and 100 mg/kg resulting in 49%, 57%, and 80% tumor growth inhibition (TGI), respectively. In comparison, efficacy with the MEK inhibitor, cobimetinib (GDC-0973), at a clinically relevant dose of 7.5 mg/kg (po, q.d.) resulted in 58% TGI. There was no observed body weight loss with treatment by **22** in this study.

Preclinical safety findings for compound **22** were consistent with those of other MEK and ERK inhibitors, namely, phosphorus dysregulation with soft tissue mineralization, decreased albumin levels, and skin toxicity in rats and gastrointestinal toxicity in dogs.[27] On the basis of the favorable
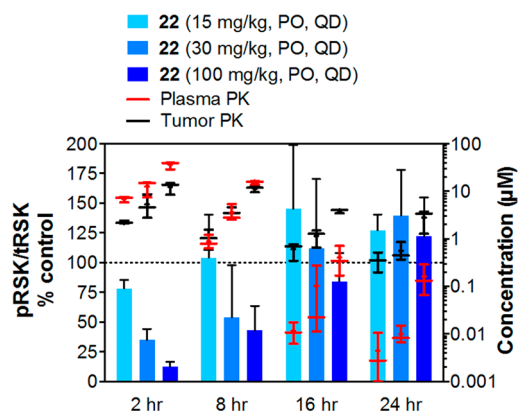
Figure 7. HCT116 study PK/PD analysis with compound **22**: PK/PD data for **22** in the HCT116 mouse xenograft model. HCT116 tumors were established in nude mice to a tumor volume of 400−600 mm³. Mice were were treated with a single oral dose of **22** at 15, 30, or 100 mg/kg versus vehicle control alone (40% PEG400/60% (10% HPβCD)) followed by tumor and plasma collection at 2, 8, 16, and 24 h postdose. Tumor levels of phosphorylated p90RSK (pRSK) relative total p90RSK (tRSK) were measured by quantitative Western blot and were normalized to vehicle control at 2 h postdose (set to 100%). Plasma and tumor concentrations were measured by LC−MS.
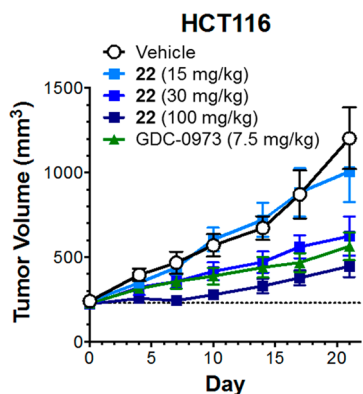
Figure 8. HCT116 mouse xenograft data with compound **22**.

efficacy and tolerability profile reported herein, compound **22** (GDC-0994) was advanced into human clinical trials.

A first-in-human, phase 1 dose escalation study was conducted in patients with locally advanced or metastatic solid tumors. Compound **22** (mesylate) was administered orally once daily as powder in capsule on a 21-day on/7-day off schedule. The plasma concentration vs time PK profiles of 50, 100, and 200 mg (three patients each) at steady state are shown in Figure 9. In general, exposures increased with dose from 50 to 200 mg.
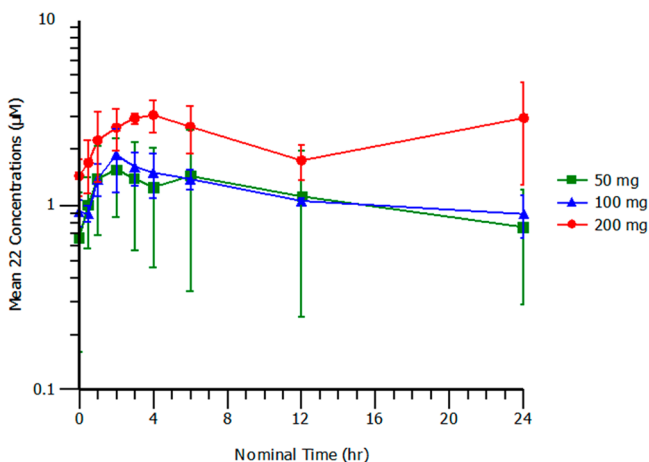

Figure 9. Mean **22** ($\pm$SD) human PK concentrations at steady state by dose.

In summary, targeting the RAS-RAF-MEK-ERK pathway has given rise to a number of FDA-approved medicines to treat various cancers. Inhibition of ERK1/2 has not been as well explored as inhibition of RAFs and MEK. Nonetheless, targeting the ERK node in the MAPK pathway is rationalized by ERKs acting as the effector kinases for the MAPK pathway and ERK phosphorylation being a central feature in therapeutic resistance. The addition of potent and selective ERK inhibitors further enables the rational targeting of multiple nodes in the MAPK pathway in order to achieve maximal efficacy. Previously, we reported compound **6** to have many desirable traits as an ERK inhibitor, but the projected human dose based on preclinical PK and efficacy studies was unacceptably high. Hence, a campaign to lower the predicted dose using a combination of improved potency and/or PK was launched. Replacement of the metabolically labile THP ring of **6** with an *N*-methylpyrazole as in compound **22** led to a compound

requiring approximately 10-fold lower total concentration and projected human dose relative to **6** to achieve target coverage. On the basis of preclinical PK/PD and efficacy experiments, coupled with a relatively safe profile in tolerability studies, compound **22** was advanced into human clinical trials. Human PK data with **22** support the predicted low clearance and feasibility of attaining target coverage at achievable doses.

■ EXPERIMENTAL SECTION

General Methods. Melting points were determined with a DSC Q100 instrument, and HRMS was conducted with a Dionex LC Ultimate3000 and ThermoScientific Q Exactive orbitrap mass spectrometer. Samples were prepared in a mixture of MeOH/acetonitrile/water (4:4:1 v/v/v) with 200 μM concentration for high resolution LCMS analysis. Samples of 5 μL were injected into the LCMS system and were analyzed by 10 min gradient HPLC and HRMS with electrospray ionization. Bruker instruments (400 and 500 MHz) were used for NMR characterization. Compounds in Table 1 were prepared by the method previously described for **6**.[21] All final compounds were purified to >95% chemical purity, as assayed by HPLC (Waters Acquity UPLC column, 21 mm × 50 mm, 1.7 μm) with a gradient of 0−90% acetonitrile (containing 0.038% TFA) in 0.1% aqueous TFA, with UV detection at λ = 254 and 210 nm and with CAD detection with an ESA Corona detector. Protein expression, purification, and crystallization of CDK2 and ERK2 were performed by the methods previously described.[21,23]

General Procedure for Preparation of Compounds in Table 2. To a solution of compound **8** (1 equiv) and the pyrazole (2 equiv) in DMF (0.03 M) was added sodium hydride (2.5 equiv, 60% dispersion in mineral oil). The mixture was stirred at room temperature or heated in a sealed tube until the addition was complete. The mixture was partitioned between EtOAc and water, the phases were separated, the aqueous phase was extracted with EtOAc, the combined organic phases were dried (Na_2SO_4) and concentrated. To the residue in EtOAc (0.02 M) was added a saturated solution of HCl in EtOAc. The mixture was stirred until complete (∼15 min), concentrated, and purified by HPLC.

(*S*)-1-(1-(4-Chloro-3-fluorophenyl)-2-hydroxyethyl)-4-(2-(2-methylpyridin-4-ylamino)pyrimidin-4-yl)pyridin-2(1*H*)-one, 9. ^{1}H NMR (400 MHz, DMSO-d_6) δ 10.16 (s, 1H), 8.72 (d, *J* = 5.1 Hz, 1H), 8.26 (d, *J* = 5.6 Hz, 1H), 7.98 (d, *J* = 7.3 Hz, 1H), 7.61 (ddd, *J* = 16.2, 9.5, 4.4 Hz, 4H), 7.45 (dd, *J* = 10.6, 1.7 Hz, 1H), 7.20 (dd, *J* = 20.6, 5.1 Hz, 2H), 6.97 (dd, *J* = 7.3, 2.0 Hz, 1H), 5.99 (dd, *J* = 7.8, 5.6 Hz, 1H), 5.34 (s, 1H), 4.19 (dd, *J* = 11.7, 8.1 Hz, 1H), 4.05 (d, *J* = 5.6 Hz, 1H), 2.42 (s, 3H). *m/z* (APCI-pos) M + 1 = 452.2.

(*S*)-1-(1-(4-Chloro-3-fluorophenyl)-2-hydroxyethyl)-4-(2-(1-methyl-1*H*-pyrazol-4-ylamino)pyrimidin-4-yl)pyridin-2(1*H*)-one, 10. ^{1}H NMR (400 MHz, DMSO-d_6) δ 9.61 (s, 1H), 8.55 (d, *J* = 5.0 Hz, 1H), 7.93 (d, *J* = 7.3 Hz, 1H), 7.87 (s, 1H), 7.64−7.52 (m, 2H), 7.45 (dd, *J* = 10.6, 1.9 Hz, 1H), 7.31 (d, *J* = 5.1 Hz, 1H), 7.21−7.14 (m, 2H), 6.93 (dd, *J* = 7.3, 1.8 Hz, 1H), 5.99 (dd, *J* = 7.7, 5.5 Hz, 1H), 5.34 (t, *J* = 5.3 Hz, 1H), 4.23−4.13 (m, 1H), 4.10−4.01 (m, 1H), 3.82 (s, 3H). *m/z* (APCI-pos) M + 1 = 441.1.

(*S*)-1-(1-(4-Chloro-3-fluorophenyl)-2-hydroxyethyl)-4-(2-(1,5-dimethyl-1*H*-pyrazol-4-ylamino)pyrimidin-4-yl)pyridin-2(1*H*)-one, 11. ^{1}H NMR (400 MHz, DMSO-d_6) δ 8.87 (s, 1H), 8.47 (d, *J* = 4.9 Hz, 1H), 7.90 (d, *J* = 7.3 Hz, 1H), 7.57 (dd, *J* = 17.1, 9.0 Hz, 2H), 7.49−7.38 (m, 1H), 7.27 (d, *J* = 5.1 Hz, 1H), 7.19−7.05 (m, 2H), 6.84 (t, *J* = 15.6 Hz, 1H), 5.97 (dd, *J* = 7.8, 5.6 Hz, 1H), 5.32 (t, *J* = 5.3 Hz, 1H), 4.15 (ddd, *J* = 13.4, 7.9, 5.7 Hz, 1H), 4.03 (dt, *J* = 21.4, 7.5 Hz, 1H), 3.71 (d, *J* = 9.7 Hz, 3H), 2.17 (d, *J* = 8.2 Hz, 3H). *m/z* (APCI-pos) M + 1 = 455.1.

(*S*)-1-(1-(4-Chloro-3-fluorophenyl)-2-hydroxyethyl)-4-(2-(1,3-dimethyl-1*H*-pyrazol-4-ylamino)pyrimidin-4-yl)pyridin-2(1*H*)-one, 12. ^{1}H NMR (400 MHz, DMSO-d_6) δ 8.90 (s, 1H), 8.50 (d, *J* = 5.1 Hz, 1H), 7.91 (d, *J* = 7.3 Hz, 1H), 7.80 (s, 1H), 7.64−7.53 (m, 1H), 7.43 (dt, *J* = 19.1, 9.5 Hz, 1H), 7.28 (dd, *J* = 9.7, 5.1 Hz, 1H), 7.21−7.07 (m, 2H), 6.89 (d, *J* = 5.9 Hz, 1H), 6.04−5.92 (m, 1H), 5.34

(t, J = 5.2 Hz, 1H), 4.24−4.10 (m, 1H), 4.10−3.97 (m, 1H), 3.80−3.70 (m, 3H), 2.11 (s, 3H). m/z (APCI-pos) M + 1 = 455.1.

(*S*)-1-(1-(4-Chloro-3-fluorophenyl)-2-hydroxyethyl)-4-(2-(3-ethyl-1-methyl-1*H*-pyrazol-4-ylamino)pyrimidin-4-yl)pyridin-2(1*H*)-one, 13. ^{1}H NMR (400 MHz, DMSO-d_6) δ 8.85 (s, 1H), 8.48 (t, J = 8.0 Hz, 1H), 7.91 (d, J = 7.3 Hz, 1H), 7.79 (s, 1H), 7.58 (t, J = 8.1 Hz, 1H), 7.49−7.38 (m, 1H), 7.27 (t, J = 5.6 Hz, 1H), 7.21−7.05 (m, 2H), 6.88 (d, J = 6.6 Hz, 1H), 5.98 (dd, J = 7.8, 5.5 Hz, 1H), 5.33 (t, J = 5.2 Hz, 1H), 4.16 (ddd, J = 13.4, 7.9, 5.6 Hz, 1H), 4.11−3.96 (m, 1H), 3.75 (d, J = 3.9 Hz, 3H), 2.54 (dd, J = 15.1, 7.5 Hz, 2H), 1.11 (dd, J = 8.8, 6.3 Hz, 3H). m/z (APCI-pos) M + 1 = 469.1.

(*S*)-1-(1-(4-Chloro-3-fluorophenyl)-2-hydroxyethyl)-4-(2-(1-ethyl-3-methyl-1*H*-pyrazol-4-ylamino)pyrimidin-4-yl)pyridin-2(1*H*)-one, 14. ^{1}H NMR (400 MHz, DMSO-d_6) δ 8.89 (s, 1H), 8.50 (d, J = 5.1 Hz, 1H), 7.91 (t, J = 5.3 Hz, 1H), 7.84 (s, 1H), 7.58 (t, J = 8.1 Hz, 1H), 7.43 (dd, J = 10.6, 1.9 Hz, 1H), 7.28 (d, J = 5.1 Hz, 1H), 7.15 (dd, J = 9.6, 7.9 Hz, 2H), 6.88 (d, J = 6.6 Hz, 1H), 5.97 (dd, J = 7.8, 5.4 Hz, 1H), 5.32 (t, J = 5.1 Hz, 1H), 4.21−4.12 (m, 1H), 4.06−3.99 (m, 3H), 2.12 (s, 3H), 1.35 (t, J = 7.2 Hz, 3H). m/z (APCI-pos) M + 1 = 469.1.

(*S*)-1-(1-(4-Chloro-3-fluorophenyl)-2-hydroxyethyl)-4-(2-(1-ethyl-1*H*-pyrazol-4-ylamino)pyrimidin-4-yl)pyridin-2(1*H*)-one, 15. ^{1}H NMR (400 MHz, DMSO-d_6) δ 9.59 (s, 1H), 8.62−8.51 (m, 1H), 7.97−7.88 (m, 2H), 7.59 (t, J = 8.1 Hz, 2H), 7.45 (dd, J = 10.5, 1.6 Hz, 1H), 7.30 (d, J = 5.1 Hz, 1H), 7.16 (t, J = 5.0 Hz, 2H), 6.93 (dd, J = 7.2, 1.6 Hz, 1H), 6.02−5.96 (m, 1H), 5.33 (s, 1H), 4.23−4.02 (m, 4H), 1.36 (t, J = 7.3 Hz, 3H). m/z (APCI-pos) M + 1 = 455.1.

(*S*)-1-(1-(4-Chloro-3-fluorophenyl)-2-hydroxyethyl)-4-(2-(1-isopropyl-1*H*-pyrazol-4-ylamino)pyrimidin-4-yl)pyridin-2(1*H*)-one, 16. ^{1}H NMR (400 MHz, DMSO-d_6) δ 9.58 (s, 1H), 8.55 (d, J = 5.0 Hz, 1H), 7.96−7.89 (m, 2H), 7.59 (t, J = 8.1 Hz, 2H), 7.45 (dd, J = 10.6, 1.7 Hz, 1H), 7.30 (d, J = 5.1 Hz, 1H), 7.22−7.13 (m, 2H), 6.92 (dd, J = 7.3, 1.8 Hz, 1H), 6.04−5.94 (m, 1H), 5.33 (t, J = 5.2 Hz, 1H), 4.46 (dt, J = 13.3, 6.6 Hz, 1H), 4.21−4.13 (m, 1H), 4.10−4.02 (m, 1H), 1.41 (d, J = 6.7 Hz, 6H). m/z (APCI-pos) M + 1 = 469.1.

(*S*)-1-(1-(4-Chloro-3-fluorophenyl)-2-hydroxyethyl)-4-(2-(3-methyl-1*H*-pyrazol-4-ylamino)pyrimidin-4-yl)pyridin-2(1*H*)-one, 17. ^{1}H NMR (400 MHz, DMSO-d_6) δ 12.28 (d, J = 50.5 Hz, 1H), 8.87 (s, 1H), 8.49 (s, 1H), 7.91 (d, J = 7.3 Hz, 1H), 7.65 (dd, J = 64.2, 56.0 Hz, 2H), 7.43 (dd, J = 10.6, 2.0 Hz, 1H), 7.27 (d, J = 5.1 Hz, 1H), 7.21−7.06 (m, 2H), 6.87 (d, J = 6.6 Hz, 1H), 5.98 (dd, J = 7.7, 5.5 Hz, 1H), 5.32 (t, J = 5.3 Hz, 1H), 4.23−4.11 (m, 1H), 4.11−4.00 (m, 1H), 2.16 (s, 3H). m/z (APCI-pos) M + 1 = 444.1.

(*S*)-1-(1-(4-Chloro-3-fluorophenyl)-2-hydroxyethyl)-4-(2-(3,5-dimethyl-1*H*-pyrazol-4-ylamino)pyrimidin-4-yl)pyridin-2(1*H*)-one, 18. ^{1}H NMR (400 MHz, DMSO-d_6) δ 12.04 (s, 1H), 8.48 (d, J = 34.0 Hz, 2H), 7.88 (d, J = 6.9 Hz, 1H), 7.57 (t, J = 8.1 Hz, 1H), 7.42 (dd, J = 10.5, 1.9 Hz, 1H), 7.24 (d, J = 5.1 Hz, 1H), 7.14 (d, J = 8.3 Hz, 1H), 7.04 (s, 1H), 6.79 (s, 1H), 6.01−5.91 (m, 1H), 5.31 (t, J = 5.2 Hz, 1H), 4.14 (s, 1H), 4.08−3.99 (m, 1H), 2.13−1.93 (m, 6H). m/z (APCI-pos) M + 1 = 455.1.

(*S*)-1-(1-(4-Chloro-3-fluorophenyl)-2-hydroxyethyl)-4-(2-((1-methyl-3-(trifluoromethyl)-1*H*-pyrazol-4-yl)amino)pyrimidin-4-yl)pyridin-2(1*H*)-one, 19. ^{1}H NMR (400 MHz, DMSO-d_6) δ 8.90 (s, 1H), 8.52 (d, J = 5.0 Hz, 1H), 8.07 (d, J = 10.3 Hz, 1H), 7.89 (d, J = 7.3 Hz, 1H), 7.57 (t, J = 8.1 Hz, 1H), 7.42 (ddd, J = 23.6, 22.8, 8.8 Hz, 2H), 7.23−7.03 (m, 2H), 6.84 (t, J = 5.7 Hz, 1H), 5.98 (dd, J = 12.8, 7.3 Hz, 1H), 5.31 (s, 1H), 4.14 (d, J = 8.3 Hz, 1H), 4.05 (s, 1H), 3.97−3.85 (m, 3H). m/z (APCI-pos) M + 1 = 509.1.

(*S*)-4-(2-((1*H*-Pyrazol-5-yl)amino)pyrimidin-4-yl)-1-(1-(4-chloro-3-fluorophenyl)-2-hydroxyethyl)pyridin-2(1*H*)-one, 20. ^{1}H NMR (400 MHz, DMSO-d_6) δ 8.95 (d, J = 5.2 Hz, 1H), 8.06−7.91 (m, 2H), 7.59 (t, J = 8.1 Hz, 1H), 7.44 (dd, J = 9.2, 6.1 Hz, 2H), 7.25 (d, J = 1.9 Hz, 1H), 7.18 (d, J = 8.4 Hz, 1H), 6.97 (dd, J = 7.3, 1.9 Hz, 1H), 6.72 (s, 2H), 6.04−5.94 (m, 1H), 5.46 (d, J = 1.6 Hz, 1H), 5.34 (t, J = 5.2 Hz, 1H), 4.24−4.12 (m, 1H), 4.11−4.00 (m, 1H). m/z (APCI-pos) M + 1 = 427.1.

(*S*)-1-(1-(4-Chloro-3-fluorophenyl)-2-hydroxyethyl)-4-(2-((1-methyl-1*H*-pyrazol-3-yl)amino)pyrimidin-4-yl)pyridin-2(1*H*)-one, 21. ^{1}H NMR (400 MHz, DMSO-d_6) δ 9.90 (s, 1H), 8.56 (d, J = 5.1 Hz, 1H), 7.92 (t, J = 9.9 Hz, 1H), 7.63−7.54 (m, 2H), 7.45 (dd, J = 10.6, 2.0 Hz, 1H), 7.37 (d, J = 5.1 Hz, 1H), 7.17 (dt, J = 4.9, 2.4 Hz, 2H), 6.92 (dd, J = 7.3, 2.0 Hz, 1H), 6.62 (d, J = 2.2 Hz, 1H), 5.99 (dd, J = 7.9, 5.5 Hz, 1H), 5.36−5.29 (m, 1H), 4.23−4.12 (m, 1H), 4.10−4.01 (m, 1H), 3.76 (s, 3H). m/z (APCI-pos) M + 1 = 444.1.

(*S*)-1-(1-(4-Chloro-3-fluorophenyl)-2-hydroxyethyl)-4-(2-((1-methyl-1*H*-pyrazol-5-yl)amino)pyrimidin-4-yl)pyridin-2(1*H*)-one, 22. mp = 304.4 °C, [$α$]$_D^{23}$ +113.8 (c 0.29, MeOH); IR 1660, 1582, 1557 cm^{-1}; ^{1}H NMR (500 MHz, DMSO-d_6) δ 9.69−9.52 (s, 1H), 8.69−8.49 (d, J = 5.1 Hz, 1H), 8.09−7.77 (d, J = 7.3 Hz, 1H), 7.61−7.56 (t, J = 8.1 Hz, 1H), 7.50−7.47 (d, J = 5.1 Hz, 1H), 7.46−7.42 (dd, J = 10.6, 2.0 Hz, 1H), 7.38−7.36 (d, J = 1.9 Hz, 1H), 7.22−7.08 (m, 2H), 6.98−6.79 (dd, J = 7.3, 2.1 Hz, 1H), 6.35−6.23 (d, J = 1.9 Hz, 1H), 6.06−5.90 (dd, J = 8.1, 5.4 Hz, 1H), 5.40−5.23 (d, J = 5.2 Hz, 1H), 4.24−3.97 (m, 2H), 3.80−3.56 (s, 3H); ^{13}C NMR (101 MHz, DMSO-d_6) δ 162.18, 161.53, 160.88, 160.55, 157.59 (d, J_{CF} = 246.83 Hz), 147.19, 140.09 (d, J_{CF} = 6.47 Hz), 138.30, 137.75, 137.42, 131.20, 125.53 (d, J_{CF} = 3.45 Hz), 119.29 (d, J_{CF} = 17.45 Hz), 117.74, 116.61 (d, J_{CF} = 21.68 Hz), 109.68, 103.34, 99.36, 61.24, 59.20, 35.93. HRMS (ESI): m/z [M + H]$^+$ calcd for $C_{21}H_{18}ClFN_6O_2$, 441.1242; found, 441.1230.

(*S*)-1-(1-(4-Chloro-3-fluorophenyl)-2-hydroxyethyl)-4-(2-((1-ethyl-1*H*-pyrazol-5-yl)amino)pyrimidin-4-yl)pyridin-2(1*H*)-one, 23. ^{1}H NMR (500 MHz, DMSO-d_6) δ 8.64−8.52 (d, J = 5.1 Hz, 1H), 7.98−7.87 (d, J = 7.4 Hz, 1H), 7.66−7.52 (t, J = 8.1 Hz, 1H), 7.47−7.45 (d, J = 5.1 Hz, 1H), 7.45−7.41 (dd, J = 10.5, 2.0 Hz, 1H), 7.40−7.38 (d, J = 1.9 Hz, 1H), 7.21−7.05 (m, 2H), 6.92−6.77 (dd, J = 7.3, 2.0 Hz, 1H), 6.33−6.18 (d, J = 1.8 Hz, 1H), 6.03−5.90 (dd, J = 8.0, 5.5 Hz, 1H), 4.24−4.07 (dd, J = 11.8, 8.2 Hz, 1H), 4.11−3.93 (q, J = 7.0 Hz, 3H), 1.41−1.13 (t, J = 7.2 Hz, 3H). m/z (APCI-pos) M + 1 = 455.1.

(*S*)-1-(1-(4-Chloro-3-fluorophenyl)-2-hydroxyethyl)-4-(2-((1,3-dimethyl-1*H*-pyrazol-5-yl)amino)pyrimidin-4-yl)pyridin-2(1*H*)-one, 24. ^{1}H NMR (400 MHz, DMSO-d_6) δ 9.54 (s, 1H), 8.59 (d, J = 5.1 Hz, 1H), 7.92 (t, J = 9.6 Hz, 1H), 7.58 (t, J = 8.1 Hz, 1H), 7.45 (dd, J = 11.5, 7.9 Hz, 2H), 7.20−7.08 (m, 2H), 6.87 (d, J = 7.3 Hz, 1H), 6.04 (s, 1H), 6.02−5.92 (m, 1H), 5.34 (t, J = 5.2 Hz, 1H), 4.24−4.10 (m, 1H), 4.10−4.00 (m, 1H), 3.59 (s, 3H), 2.12 (s, 3H). m/z (APCI-pos) M + 1 = 455.1.

(*S*)-1-(1-(4-Chloro-3-fluorophenyl)-2-hydroxyethyl)-4-(2-((1-ethyl-3-methyl-1*H*-pyrazol-5-yl)amino)pyrimidin-4-yl)pyridin-2(1*H*)-one, 25. ^{1}H NMR (400 MHz, DMSO-d_6) δ 9.44 (s, 1H), 8.57 (d, J = 5.1 Hz, 1H), 7.92 (d, J = 7.3 Hz, 1H), 7.58 (t, J = 8.1 Hz, 1H), 7.49−7.37 (m, 2H), 7.14 (dd, J = 13.4, 4.8 Hz, 2H), 6.86 (d, J = 7.2 Hz, 1H), 6.03 (s, 1H), 6.00−5.90 (m, 1H), 5.31 (t, J = 5.2 Hz, 1H), 4.22−4.09 (m, 1H), 4.08−3.99 (m, 1H), 3.94 (q, J = 7.2 Hz, 2H), 2.14 (s, 3H), 1.25 (t, J = 7.2 Hz, 3H). m/z (APCI-pos) M + 1 = 469.1.

(*S*)-1-(1-(4-Chloro-3-fluorophenyl)-2-hydroxyethyl)-4-(2-((3-ethyl-1-methyl-1*H*-pyrazol-5-yl)amino)pyrimidin-4-yl)pyridin-2(1*H*)-one, 26. ^{1}H NMR (400 MHz, DMSO-d_6) δ 9.48 (s, 1H), 8.58 (d, J = 5.1 Hz, 1H), 7.92 (d, J = 7.3 Hz, 1H), 7.57 (t, J = 8.1 Hz, 1H), 7.49−7.37 (m, 2H), 7.15 (dd, J = 8.6, 6.0 Hz, 2H), 6.86 (dd, J = 7.3, 1.9 Hz, 1H), 6.07 (s, 1H), 5.97 (dd, J = 7.8, 5.6 Hz, 1H), 5.30 (s, 1H), 4.16 (s, 1H), 4.04 (d, J = 11.9 Hz, 1H), 3.60 (s, 3H), 2.52 (d, J = 6.1 Hz, 1H), 2.47 (s, 1H), 1.16 (t, J = 7.6 Hz, 3H). m/z (APCI-pos) M + 1 = 469.1.

(*S*)-1-(1-(4-Chloro-3-fluorophenyl)-2-hydroxyethyl)-4-(2-((1,4-dimethyl-1*H*-pyrazol-5-yl)amino)pyrimidin-4-yl)pyridin-2(1*H*)-one, 27. ^{1}H NMR (400 MHz, DMSO-d_6) δ 9.21 (s, 1H), 8.54 (d, J = 5.1 Hz, 1H), 7.90 (d, J = 7.3 Hz, 1H), 7.57 (t, J = 8.1 Hz, 1H), 7.41 (dd, J = 7.8, 3.4 Hz, 2H), 7.25 (s, 1H), 7.14 (d, J = 8.4 Hz, 1H), 7.07 (s, 1H), 6.79 (s, 1H), 6.02−5.88 (m, 1H), 5.30 (t, J = 5.1 Hz, 1H), 4.14 (dd, J = 15.2, 9.9 Hz, 1H), 4.08−3.96 (m, 1H), 3.58 (s, 3H), 1.83 (s, 3H). m/z (APCI-pos) M + 1 = 455.1.

(*S*)-1-(1-(4-Chloro-3-fluorophenyl)-2-hydroxyethyl)-4-(2-((1-methyl-3-(trifluoromethyl)-1*H*-pyrazol-5-yl)amino)pyrimidin-4-yl)pyridin-2(1*H*)-one, 28. ^{1}H NMR (400 MHz, DMSO-d_6) δ 9.90 (s, 1H), 8.65 (d, J = 5.1 Hz, 1H), 7.94 (d, J = 7.3 Hz, 1H), 7.57 (dd, J = 15.4, 6.7 Hz, 2H), 7.43 (dd, J = 10.6, 1.9 Hz, 1H), 7.16 (dd, J = 9.7, 1.6 Hz, 2H), 6.86 (dd, J = 7.3, 1.9 Hz, 1H), 6.74 (s, 1H), 5.97 (dd, J = 7.8, 5.6 Hz, 1H), 5.30 (t, J = 5.2 Hz, 1H), 4.17 (ddd, J = 13.4, 8.0, 5.7

Hz, 1H), 4.09–3.97 (m, 1H), 3.80 (s, 3H). *m/z* (APCI-pos) M + 1 = 509.1.

ASSOCIATED CONTENT

ⓢ Supporting Information

The Supporting Information is available free of charge on the ACS Publications website at DOI: 10.1021/acs.jmedchem.6b00389.

> Experimental procedures for the crystal structure determination of ERK2 and CDK2 complexes with **22** (PDF)
>
> Molecular formula strings (CSV)

AUTHOR INFORMATION

Corresponding Author

*Phone: 650-225-7732. E-mail: schwarz.jacob@gene.com.

Notes

The authors declare no competing financial interest.

ABBREVIATIONS USED

MAPK, mitogen-activated protein kinase; LC–MS, liquid chromatography–mass spectrometry; TBAF, tetrabutylammonium fluoride; RSK, ribosomal s6 kinase; CYP, cytochrome P450; CDK, cyclin-dependent kinase; PK, pharmacokinetic; PD, pharmacodynamics; SAR, structure–activity relationship; MDCK, Madin–Darby canine kidney; po, per os (by mouth); iv, intravenous; HCT, human colorectal carcinoma; DMF, dimethylformamide; EtOAc, ethyl acetate; MeOH, methanol

REFERENCES

(1) Roberts, P. J.; Der, C. J. Targeting the Raf-MEK-ERK mitogen-activated protein kinase cascade for the treatment of cancer. *Oncogene* **2007**, *26*, 3291–3310.

(2) Seger, R.; Krebs, E. G. The MAPK signaling cascade. *FASEB J.* **1995**, *9*, 726–735.

(3) Lewis, T. S.; Shapiro, P. S.; Ahn, N. G. Signal transduction through MAP kinase cascades. *Adv. Cancer Res.* **1998**, *74*, 49–139.

(4) Pearson, G.; Robinson, F.; Gibson, T. B.; Xu, B.; Karandikar, M.; Berman, K.; Cobb, M. H. Mitogen-activated protein (MAP) kinase pathways: regulation and physiological functions. *Endocr. Rev.* **2001**, *22*, 153–183.

(5) Flaherty, K. T.; Yasothan, U.; Kirkpatrick, P. Vemurafenib. *Nat. Rev. Drug Discovery* **2011**, *10*, 811–812.

(6) Ballantyne, A. D.; Garnock-Jones, K. P. Dabrafenib: first global approval. *Drugs* **2013**, *73*, 1367–1376.

(7) Wright, C. J. M.; McCormack, P. L. Trametinib: first global approval. *Drugs* **2013**, *73*, 1245–1254.

(8) Garnock-Jones, K. P. Cobimetinib: first global approval. *Drugs* **2015**, *75*, 1823–1830.

(9) Moriceau, G.; Hugo, W.; Hong, A.; Shi, H.; Kong, X.; Yu, C. C.; Koya, R. C.; Samatar, A. A.; Khanlou, N.; Braun, J.; Ruchalski, K.; Seifert, H.; Larkin, J.; Dahlman, K. B.; Johnson, D. B.; Algazi, A.; Sosman, J. A.; Ribas, A.; Lo, R. S. Tunable-combinatorial mechanisms of acquired resistance limit the efficacy of BRAF/MEK cotargeting but result in melanoma drug addiction. *Cancer Cell* **2015**, *27*, 240–256.

(10) Sale, M. J.; Cook, S. J. Intrinsic and acquired resistance to MEK1/2 inhibitors in cancer. *Biochem. Soc. Trans.* **2014**, *42*, 776–783.

(11) Chapman, P. B.; Solit, D. B.; Rosen, N. Combination of RAF and MEK inhibition for the treatment of BRAF-mutated melanoma: feedback is not encouraged. *Cancer Cell* **2014**, *26*, 603–604.

(12) Yu, Z.; Ye, S.; Hu, G.; Lv, M.; Tu, Z.; Zhou, K.; Li, Q. The RAF-MEK-ERK pathway: targeting ERK to overcome obstacles of effective cancer therapy. *Future Med. Chem.* **2015**, *7*, 269–289.

(13) Goetz, E. M.; Ghandi, M.; Treacy, D. J.; Wagle, N.; Garraway, L. A. ERK mutations confer resistance to mitogen-activated protein kinase pathway inhibitors. *Cancer Res.* **2014**, *74*, 7079–7089.

(14) Yap, J. L.; Worlikar, S.; MacKerell, A. D., Jr.; Shapiro, P.; Fletcher, S. Small-molecule inhibitors of the ERK signaling pathway: towards novel anticancer therapeutics. *ChemMedChem* **2011**, *6*, 38–48.

(15) Aronov, A. M.; Baker, C.; Bemis, G. W.; Cao, J.; Chen, G.; Ford, P. J.; Germann, U. A.; Green, J.; Hale, M. R.; Jacobs, M.; Janetka, J. W.; Maltais, F.; Martinez-Botella, G.; Namchuk, M. N.; Straub, J.; Tang, Q.; Xie, X. Flipped out: structure-guided design of selective pyrazolylpyrrole ERK inhibitors. *J. Med. Chem.* **2007**, *50*, 1280–1287.

(16) Biomed Valley Discoveries, BVD-523. https://biomed-valley.com/portfolio/bvd-523.

(17) Bagdanoff, J. T.; Jain, R.; Han, W.; Zhu, S.; Madiera, A.-M.; Lee, P. S.; Ma, X.; Poon, D. Tetrahydropyrrolo-diazepenones as inhibitors of ERK2 kinase. *Bioorg. Med. Chem. Lett.* **2015**, *25*, 3788–3792.

(18) Morris, E. J.; Jha, S.; Restaino, C. R.; Dayananth, P.; Zhu, H.; Cooper, A.; Carr, D.; Deng, Y.; Jin, W.; Black, S.; Long, B.; Liu, J.; DiNunzio, E.; Windsor, W.; Zhang, R.; Zhao, S.; Angagaw, M. H.; Pinheiro, E. M.; Desai, J.; Xiao, L.; Shipps, G.; Hruza, A.; Wang, J.; Kelly, J.; Paliwal, S.; Gao, X.; Babu, B. S.; Zhu, L.; Daublain, P.; Zhang, L.; Lutterbach, B. A.; Pelletier, M. R.; Philippar, U.; Siliphaivanh, P.; Witter, D.; Kirschmeier, P.; Bishop, W. R.; Hicklin, D.; Gilliland, D. G.; Jayaraman, L.; Zawel, L.; Fawell, S.; Samatar, A. A. Discovery of a novel ERK inhibitor with activity in models of acquired resistance to BRAF and MEK inhibitors. *Cancer Discovery* **2013**, *3*, 742–750.

(19) Ward, R. A.; Colclough, N.; Challinor, M.; Debreczeni, J. E.; Eckersley, K.; Fairley, G.; Feron, L.; Flemington, V.; Graham, C. R.; Greenwood, R.; Hopcroft, P.; Howard, T. D.; James, M.; Jones, C. D.; Jones, C. R.; Renshaw, J.; Roberts, K.; Snow, L.; Tonge, M.; Yeung, K. Structure-guided design of highly selective and potent covalent inhibitors of ERK1/2. *J. Med. Chem.* **2015**, *58*, 4790–4801.

(20) Blake, J. F.; Gaudino, J. J.; De Meese, J.; Mohr, P.; Chicarelli, M.; Tian, H.; Garrey, R.; Thomas, A.; Siedem, C. S.; Welch, M. B.; Kolakowski, G.; Kaus, R.; Burkard, M.; Martinson, M.; Chen, H.; Dean, B.; Dudley, D. A.; Gould, S. E.; Pacheco, P.; Shahidi-Latham, S.; Wang, W.; West, K.; Yin, J.; Moffat, J.; Schwarz, J. B. Discovery of 5,6,7,8-tetrahydropyrido[3,4-d]pyrimidine inhibitors of Erk2. *Bioorg. Med. Chem. Lett.* **2014**, *24*, 2635–2639.

(21) Ren, L.; Grina, J.; Moreno, D.; Blake, J. F.; Gaudino, J. J.; Garrey, R.; Metcalf, A. T.; Burkard, M.; Martinson, M.; Rasor, K.; Chen, H.; Dean, B.; Gould, S. E.; Pacheco, P.; Shahidi-Latham, S.; Yin, J.; West, K.; Wang, W.; Moffat, J. G.; Schwarz, J. B. Discovery of highly potent, selective and efficacious small molecule inhibitors of ERK1/2. *J. Med. Chem.* **2015**, *58*, 1976–1991.

(22) The projected human dose for **6** was calculated using the predicted human clearance from simple allometry and the AUC$_{last}$ for a dose that effected ∼70% TGI.

(23) Blake, J. F.; Chen, H.; Chicarelli, M. J.; Demeese, J.; Garrey, R.; Gaudino, J. J.; Kaus, R. J.; Kolakowski, G. R.; Marlow, A. L.; Mohr, P. J.; Ren, L.; Schwarz, J.; Siedem, C. S.; Thomas, A. A.; Wallace, E.; Wenglowsky, S. M. Pyridopyrimidine derivatives as ERK inhibitors and their preparation and use for the treatment of hyperproliferative diseases. PCT Int. Appl. WO 2012118850, 2012; 251 pp.

(24) Expression, purification, and crystallization of CDK2 has been previously described: Hanan, E. J.; Eigenbrot, C.; Bryan, M. C.; Burdick, D. J.; Chan, B. K.; Chen, Y.; Dotson, J.; Heald, R. A.; Jackson, P. S.; La, H.; Lainchbury, M. D.; Malek, S.; Purkey, H. E.; Schaefer, G.; Schmidt, S.; Seward, E. M.; Sideris, S.; Tam, C.; Wang, S.; Yeap, S. K.; Yen, I.; Yin, J.; Yu, C.; Zilberleyb, I.; Heffron, T. P. Discovery of selective and noncovalent diaminopyrimdine-based inhibitors of epidermal growth factor receptor containing the T790M resistance mutation. *J. Med. Chem.* **2014**, *57*, 10176–10191.

(25) A similar strategy was employed to gain selectivity for Plk1 over CDK2: Kothe, M.; Kohls, D.; Low, S.; Coli, R.; Rennie, G. R.; Feru, F.; Kuhn, C.; Ding, Y.-H. Selectivity-determining residues in Plk1. *Chem. Biol. Drug Des.* **2007**, *70*, 540–546.

(26) The increase in concentration of **22** at 6−8 h may be due to dose/solubility limited absorption where there is continued absorption during compound transit in the gut.

(27) Diaz, D.; Allamneni, K.; Tarrant, J. M.; Lewin-Koh, S.-C.; Pai, R.; Dhawan, P.; Cain, G. R.; Kozlowski, C.; Hiraragi, H.; La, N.; Hartley, D. P.; Ding, X.; Dean, B. J.; Bheddah, S.; Dambach, D. M. Phosphorous dysregulation induced by MEK small molecule inhibitors in the rat involves blockade of FGF-23 signaling in the kidney. *Toxicol. Sci.* **2012**, *125*, 187−195.